Journal of Drug Delivery Science and Technology 92 (2024) 105337

Contents lists available at ScienceDirect

Journal of Drug Delivery Science and Technology

journal homepage: www.elsevier.com/locate/jddst

Ensuring the quality of 3D printed medicines: Integrating a balance into a pharmaceutical printer for in-line uniformity of mass testing

Carlos Bendicho-Lavilla [a,b], Lucía Rodríguez-Pombo [c], Patricija Januskaite [d], Carlos Rial [a,b], Carmen Alvarez-Lorenzo [c], Abdul W. Basit [a,b,d,*], Alvaro Goyanes [a,b,c,d,**]

[a] FABRX Ltd., Henwood House, Henwood, Ashford, Kent, TN24 8DH, UK
[b] FABRX Artificial Intelligence, Carretera de Escairón, 14, Currelos (O Saviñao), CP, 27543, Spain
[c] Departamento de Farmacología, Farmacia y Tecnología Farmacéutica, I+D Farma (GI-1645), Facultad de Farmacia, Instituto de Materiales (iMATUS) and Health Research Institute of Santiago de Compostela (IDIS), Universidade de Santiago de Compostela, 15782, Santiago de Compostela, Spain
[d] Department of Pharmaceutics, UCL School of Pharmacy, University College London, 29-39 Brunswick Square, London, WC1N 1AX, UK

ARTICLE INFO

Keywords:
Process analytical technology (PAT)
Quality control of drug products
Weight uniformity
Three-dimensional printing of formulations
Material extrusion and direct ink writing
M3DIMAKER studio

ABSTRACT

Semi-solid extrusion (SSE) 3D printing has great potential to be integrated in a clinical setting, with the use of pre-filled and disposable pharma-ink syringes meeting regulatory good manufacturing practice (GMP) requirements. Uniformity of mass testing is a critical quality attribute and is carried out by weighing a specific amount of dosage units in a single batch and finding the average mass to evaluate any deviations. However, this test for small batches of 3D printed medicines may require weighing the entire manufactured batch. To overcome this limitation, an in-line analytical balance was implemented inside a GMP pharmaceutical 3D printer, with a specialised software-controlled weighing system for the automated mass uniformity testing of the entire printed batch. Three different dose batches (n = 28) of hydrocortisone pharma-ink were 3D printed and subjected to in-line mass uniformity testing. The developed software was capable of registering the weights of all individual printlets and accurately detecting any deviations within the accepted limits. Only one printlet was outside the accepted weight range, a result of the first print often being imperfect due to the semi-solid nature of the pharma-ink. The weight results were compared against an external analytical balance, and no significant differences were found. This study is the first to integrate an analytical balance inside a pharmaceutical printer, automating the dosage form mass uniformity testing which can save time, labour, and resources, whilst improving the quality control testing of 3D printed pharmaceuticals.

1. Introduction

Additive manufacturing, also known as three-dimensional (3D) printing (3DP), involves the production of tailor-made 3D structures through digital computer-aided design (CAD) files, in a layer-by-layer manner [1–3]. 3DP has been widely investigated in the pharmaceutical field to produce unique and personalised medicines in the form of Printlets (3D printed tablets) [4–7]. Pharmaceutical 3DP can manufacture medicines in a wide range of doses, shapes, flavours, colours, drug combinations and drug release profiles, unique to each patient or disease state [8–11]. Such features make this technology favourable to numerous patient groups such as paediatrics and geriatrics, polypharmacy patients, and rare disease patients. 3DP has also been investigated as an alternative to pharmaceutical compounding, providing treatment at the point-of-care [12]. The use of 3DP would ultimately reduce dosing errors and contamination, improve the quality, and automate and accelerate the compounding process [13–15].

Among the various 3DP technologies investigated, material extrusion technologies are the most used in pharmaceutics [16]. The main extrusion-based technologies are fused deposition modelling (FDM) [17–19], direct powder extrusion (DPE) [20–22], and semi-solid extrusion (SSE) [23–25], depending on the nature of the pharma-ink (drug loaded ink - term coined for the first time by Ref. [26]). SSE 3DP uses semi-solid pharma-inks, in the form of gels or pastes, that are deposited layer-by-layer to create a solid dosage form [27–31]. Printing can be carried out at low temperatures, making it especially beneficial for

* Corresponding author. FABRX Ltd., Henwood House, Henwood, Ashford, Kent, TN24 8DH, UK.
** Corresponding author. FABRX Ltd., Henwood House, Henwood, Ashford, Kent, TN24 8DH, UK.
E-mail addresses: a.basit@ucl.ac.uk (A.W. Basit), a.goyanes@fabrx.co.uk (A. Goyanes).

https://doi.org/10.1016/j.jddst.2024.105337
Received 14 September 2023; Received in revised form 19 December 2023; Accepted 2 January 2024
Available online 2 January 2024

bioprinting applications or thermolabile drugs [32–34]. SSE is capable of producing unique dosage forms, such as chewable tablets [35,36], orodispersible films (ODFs) [37,38], medical devices [39,40], or polypills [9]. The use of Generally Recognized As Safe (GRAS) materials, no contamination through the use of disposable syringes and printheads, and easy system maintenance and cleaning are key to meeting regulatory good manufacturing practice (GMP) requirements [41]. As a result, this has been the first 3DP technology to be used in a clinical study for paediatric patients with maple syrup urine disease (MSUD) [42], and a bioequivalence study investigating 3D printed sildenafil citrate [43].

To prove that 3DP at the point-of-care is a feasible approach to personalised medicine manufacture, rigorous quality control (QC) measures must be in place to ensure optimal performance and product safety [44]. The European Pharmacopeia (Ph. Eur.) and United States Pharmacopeia (USP) have strict requirements for uniformity of dosage units, such as uniformity of content and uniformity of mass [45]. In general, conventional uniformity of mass testing for tablets in the pharmaceutical industry involves the weighing of 20 dosage forms at random from the prepared large batch and determining the average mass to confirm if any deviate from that value by a predetermined percentage. For example, in the case of tablets with an average mass of ≥250 mg, the accepted limit is 5%. This is a destructive procedure since the 20 units are removed from the batch and analysed in the QC laboratory before acceptance. As an industrial process control measure, some of the tablets prepared during the compression process are weighed in real time and the weight and deviation are recorded on the control chart. However, 3DP technology is intended to prepare small and personalised batches of medicines on demand for specific patients at the point-of care, therefore, the uniformity of mass testing may require weighing of the whole batch. With the implementation of a balance within the pharmaceutical 3D printer, mass uniformity testing of the whole printed batch could be carried out in-line. Compared to the current Ph. Eur. and USP requirements, this automatic method would control the weight of all the printlets in the batch. The use of a specialised software linked to the balance can also provide quick information on the mass of each printlet and any deviations that occur during printing. Automating the process can save time, labour and resources, whilst improving the QC testing of 3D printed pharmaceuticals.

Conventional QC measures for drug products involve quality by testing (QbT), which are often destructive in nature and include labour intensive and time-consuming techniques such as high-performance liquid chromatography (HPLC) [46]. Performing this type of testing at the point-of-care would incur higher costs in terms of time and resources as the batches produced are small and personalised for each patient. An alternative approach to QC for 3D printed dosage forms is quality by design (QbD), which involves the identification of critical quality attributes (CQAs) during manufacture. Process analytical technology (PAT) tools are emerging as techniques for analysing the key CQAs, which can be installed in-line, on-line, at-line, or off-line, supplying both qualitative and quantitative information. Examples of PAT tools already investigated with 3DP include an integrated pressure sensor in an SSE printhead which could characterise the rheological properties of the pharma-ink during printing and inform the user of the system performance [47]. Another example of integrated PAT tools is the use of near-infrared (NIR) spectroscopy for drug quantification in two-dimensional (2D) and 3D printed pharmaceuticals [26,48–53], which can be used to conduct automated and non-destructive uniformity of content tests at the point-of-care [26].

This study aimed to integrate an in-line analytical balance into a GMP pharmaceutical 3D printer and establish a software-controlled weighing procedure to enable automated mass uniformity testing. A semi-solid pharma-ink containing hydrocortisone was developed and validated using the integrated balance and 3D printer software. Three batches of printlets (n = 28) with varying doses were 3D printed and subjected to in-line mass uniformity testing. The results of these tests were compared against those obtained from an external analytical balance. Finally, the printlets were comprehensively characterised in terms of drug content, *in vitro* drug release, and physicochemical properties.

2. Materials and methods

2.1. Materials

Hydrocortisone base (MW 362.46 g/mol, Acofarma, Barcelona, Spain), Gelucire 50/13 pellets (Gattefossé, SAS, Saint-Priest, France) and glycerol anhydrous (≥99.0%, Merck, Darmstadt, Germany) were used for the preparation of the pharma-ink. Acetonitrile and methanol (HPLC grade, Sigma-Aldrich, Dorset, UK) were used as the mobile phase for the drug content assay. Hydrochloric acid (37%, Ph. Eur, Scharlau, Barcelona, Spain) was used for the preparation of the dissolution testing media. All materials were used as received.

2.2. Preparation of the pharma-ink

The developed pharma-ink consisted of 89.6% w/w Gelucire 50/13, 10% w/w glycerol, and 0.4% w/w hydrocortisone base. The excipients and the drug were mixed in a metal container and heated to 60 °C under magnetic stirring for 30 min on a heating plate. The resulting pharma-ink was then transferred to a disposable cartridge and allowed to cool at room temperature until printing.

2.3. Balance integration in the pharmaceutical 3D printer

An analytical balance was integrated into a M3DIMAKER 1 pharmaceutical 3D printer (FABRX Ltd., London, UK) (Fig. 1). The printing bed, in this case a glass platform, was positioned on top of the balance. The 3D printer system was insulated using the polycarbonate cover supplied to mitigate potential weight measurement fluctuations resulting from air currents. Additionally, the equipment was placed on an anti-vibration plate to avoid weight variations due to the vibrations produced during the printing process.

The M3DIMAKER Studio™ software (FABRX AI, Santiago de Compostela, Spain), which controls the 3D printer, was adapted to control the balance. The software interface showed the current weight being measured by the balance and added the option to remotely tare the balance. The integration of the balance led to the development of two features in the software. Firstly, the software established a relationship between the 3D models and the weight of the printed object with those 3D models through a printing and weighing process. Secondly, the software facilitated the in-line mass uniformity testing of each printed batch.

2.4. Validation of the printing process of the pharma-ink

The validation of the printing process of the pharma-ink was conducted following the M3DIMAKER Studio™ software wizard. Initially, a 3D model was selected from the software's repository, in this case, a rounded-corner cube. Subsequently, the printing parameters were configured in the software slicer (20% infill density, rectilinear fill pattern, 1 mm layer height, 2 perimeters, 0 solid layers, 15 mm/s printing speed, 5 mm filament diameter, and 1.2 mm nozzle diameter). The next step involved introducing the printing temperature (50 °C), the chosen 3DP technology (SSE), and the drug content of the pharma-ink (0.4% w/w). Finally, based on the selected printing parameters, the software sent instructions to the 3D printer to print a batch of 30 printlets arranged in 5 rows of 6 printlets each, with varying weights per row. The balance automatically measured the weight of each printlet, and the software employed internal algorithms to establish a relationship between the size, weight, dose, and printing parameters. Once a correlation was established, it was possible to input a specific target dose and the 3D model selected by the software would print the required

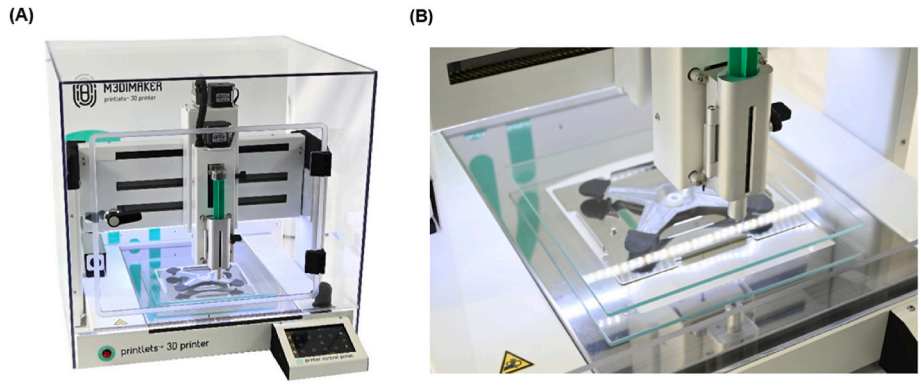

Fig. 1. Images of the balance-3D printer M3DIMAKER 1 system: (A) Full view of the printer system and (B) magnified view of the printing platform.

printlet mass.

Once the pharma-ink was successfully validated, the software saved all the data and enabled the initiation of a new print. The M3DIMAKER Studio™ allows the selection of various distributions of printlets on the printing bed, along with a range of weights or doses that can apply to either the entire batch or to each individual printlet.

2.5. 3D printing process and in-line uniformity testing

Following the validation of the printing process, three batches of 28 printlets were selected for printing, to simulate a conventional 1-month treatment for a patient with a therapeutic regimen of 1 tablet every 24 h. Additional batches were printed to carry out dissolution tests and characterization assays mentioned in the following sections. These batches contained doses of 1 mg, 2 mg, and 3 mg of hydrocortisone, respectively. Table 1 shows the theoretical dose, dimensions, and weight of the selected printlets. The pharma-ink cartridge was inserted into the SSE printhead of the M3DIMAKER 3D printer and heated at 50 °C for 15 min. The 3DP process was then initiated using the selected 3D model and the printing parameters established during the validation phase.

For the printing-weighing process, the M3DIMAKER 1 printer manufactured the printlets individually. After each printlet was complete, the SSE printhead moved up and paused for 20 s to allow the balance to stabilise. The balance reported the weight measurement for each printlet to the software, which displayed the value in the respective position of the printlet on the Printing Information tab. The balance was then automatically tared and the subsequent printlet was printed.

A mass uniformity test was conducted after manufacturing each printlet. This involved comparing the experimental weight of the printlet to its expected theoretical weight (250 mg, 500 mg, or 750 mg). If the printlet weight fell within the accepted limits, ±5% of the expected weight according to the Ph. Eur. standards, the software highlighted it in green. However, if a printlet weight deviated outside these accepted limits, the software highlighted it in red, leading to its rejection and removal from the batch after checking the weight with the external balance.

After the printing process, the dimensions of each printlet were determined using a Vernier digital caliper (SIBUR International Gmbh, Vienna, Austria). The weights reported by the integrated balance were compared with an external analytical balance (KERN PEJ model, KERN & SOHN, Balinge, Germany) to assess any weight variation that could be produced in the printing process due to measurement fluctuations. A paired student-t test was performed ($\alpha < 0.05$) using GraphPad Prism (v9.0.2, Dotmatics, Boston, USA) to determine statistical differences between the integrated and external balance. Finally, the printlets whose weight was within the accepted limits (according to the Pharmacopeia) were immediately placed in Class B X-Large amber PVC blisters (Health Care Logistics, Circleville, USA).

Table 1
Theoretical dose, dimensions, and weight of the printlets.

Dose (mg)	Width (mm)	Height (mm)	Weight (mg)
1	8.07	3.23	250
2	9.83	3.93	500
3	11.25	4.50	750

2.6. Physicochemical characterization of the printlets

2.6.1. X-ray powder diffraction (XRPD)

X-ray diffraction patterns of crystalline powder samples (hydrocortisone, Gelucire 50/13 and glycerol) were obtained in a D8 Advance diffractometer (Bruker, Billerica, MA, USA) using the Bragg-Brentano focusing geometry, equipped with a sealed X-ray tube ((CuKα1 (λ = 1.5406 Å)) and a LYNXEYE-type detector. Samples were deposited on an oriented Se(511) plate to avoid scattering noise caused by a glass support. Samples were rotated during measurement to obtain optimal peak profiles for analysis and to minimize the effect of the preferential orientation.

X-ray diffraction patterns of the pharma-ink and printlets were obtained in an Empyrean-type diffractometer (Malvern Panalytical, Malvern, UK), equipped with a five-axis goniometer (Chi-Phi-x-y-z platform). The X-rays were obtained from a sealed Cu tube of the Empyrean Cu LFFHR type (CuKα1 (λ = 1.5406 Å). The detection of X-rays from the sample was carried out with a PANalytical PIXcel-3D type area detector. The incident radiation beam was focused with a multilayer parallel beam mirror, to work with rough-non-planar surfaces.

The intensity and voltage applied were operating at 40 mA and 40 kV, respectively. The diffractograms were obtained in the 2θ angular range of 3–50°, with a step of 0.04° and a counting time of 4 s per step.

2.6.2. Thermal analysis

Differential scanning calorimetry (DSC) was used to characterise the thermal behaviour of the printlets, the pharma-ink before printing, pure hydrocortisone, and pure excipients. DSC measurements were carried out using a DSC Q100 (TA Instruments, New Castle, DE, USA) with a refrigerated cooling accessory at a heating rate of 10 °C/min. The temperature range was 0–250 °C and nitrogen was used as the purge gas, at a flow rate of 50 mL/min. All experiments were performed using non-hermetic aluminium pans, in which 1–15 mg of sample was accurately weighed using the precision balance (0.0001 mg) of TGA55 Discovery series equipment (TA Instruments, New Castle, DE, USA). Data was collected with the TA Advantage software for Q series (version 2.8) and analysed using TA Instruments Universal Analysis 2000 (version 4.5.0.5).

2.6.3. Fourier-transform infrared spectroscopy (FTIR)

The attenuated total reflectance Fourier transform infrared (ATR-

FTIR) spectra of hydrocortisone, pharma-ink, Gelucire 50/13, glycerol and printlets were collected using a Varian 670 FTIR spectrometer (Varian Inc., Palo Alto, USA). All samples were scanned between 4000 and 400 cm^{-1} at a resolution of 4 cm^{-1} for 32 scans.

2.7. Drug content determination

Samples of the different printlets were placed in a beaker (50 mL) with Milli-Q® water and were subjected to magnetic stirring (300 rpm) overnight. Samples of solution were then filtered through 0.22 μm filters (Millipore Ltd., Dublin, Ireland) and the concentration of drug was determined with HPLC-UV JASCO LC-4000 Series HPLC system (Jasco, Madrid, Spain). The assay entailed injecting 30 μL samples for analysis using a mobile phase of methanol and water (70:30 v/v) containing 1% v/v formic acid through a Symmetry 5 μm C18 column, 4.6 mm × 250 mm (Waters, Milford, Massachusetts) maintained at 30 °C. The mobile phase was pumped at a flow rate of 0.6 mL/min and the eluent was screened at a wavelength of 250 nm. Measurements were made for 28 printlets (the number of printed dosage forms in each batch) prepared for 1 mg, 2 mg, and 3 mg. The retention time was 6.5 min, and the concentration range was 0.07–160 μg/mL.

2.8. In vitro release studies

The hydrocortisone release profiles from the printlets were evaluated using a SR8-Plus Dissolution Test Station (Hanson Research, Chatsworth, CA, USA) with USP-II apparatus, connected to an Auto Plus DissoScan pump system (Hanson Research, Chatsworth, CA, USA). The paddle speed was set to 50 rpm with a temperature of 37 ± 0.5 °C. The printlets were placed in a 900 mL vessel of 0.1 M HCl (pH = 1.2) until complete dissolution to simulate gastric conditions. During the dissolution assay, samples were automatically withdrawn and filtered through 10 μm filters, and the concentration of hydrocortisone in each sample solution was determined using an in-line UV spectrophotometer (Agilent 8453, Agilent, Santa Clara, USA) at a wavelength of 250 nm. After each measurement, the samples were automatically returned to each dissolution vessel, keeping volume constant. At the end of the assay, 5 mL of sample was withdrawn from each vessel, filtered through 0.22 μm filters (Millipore Ltd., Dublin, Ireland), and analysed using HPLC to determine the final amount of drug released (method described in the previous section). Tests were conducted in triplicate under sink conditions. Data were reported throughout as mean ± standard deviation (n = 3).

3. Results and discussion

3.1. Pharma-ink development and validation of the printing process

The lipid Gelucire 50/13 was chosen as the main excipient for the development of the pharma-ink due to its favourable printability and its prior use in SSE 3DP. Hydrocortisone was selected as the model drug due to its requirements for dose personalisation [54–56]. Hydrocortisone is the recommended glucocorticoid during childhood and puberty for the treatment of cortisol deficiency (adrenal insufficiency) [57]. In clinical practice, the hydrocortisone dose is calculated based on the patient's body surface area and is commonly 8–10 mg/m^2/day, administered between 2 and 4 times a day [58]. Hydrocortisone medicines tailored to paediatric patients are scarce. As a result, hydrocortisone formulations are prepared in hospitals via pharmaceutical compounding [59]. Commercial tablets are crushed, or hydrocortisone suspensions are formulated in hospital pharmacies to comply with specific patient needs. However, pharmaceutical compounding exhibits some limitations such as being time consuming, requiring human resources, exhibiting dosing errors, and having difficulties meeting continuous dose changes [60].

The selected drug loading of the pharma-ink (0.4% w/w) was suitable to cover the dose range commonly prescribed in clinical practice. 1 mg, 2 mg and 3 mg of hydrocortisone (corresponding to a 250 mg, 500 mg and 750 mg weight, respectively) were selected as model doses to investigate the feasibility of the balance-3D printer system to carry out the mass uniformity assay similar to how it would be performed in a hospital setting. During the preparation of the pharma-ink, all excipients were mixed with the drug, resulting in the solubilization of the drug within the lipidic matrix. The obtained pharma-ink was sufficiently liquid to be manually poured into the printing cartridge. After a few minutes at room temperature, the pharma-ink solidified, forming a paste that needed to be heated to 50 °C to become printable.

To correlate the 3D model size and the weight of the printlets, the 3D model with dimensions of 10 mm × 10 mm x 4 mm was scaled to produce 5 different sizes. The recorded weights after printing ranged from 250 mg to 1,500 mg. The software established a relationship between the 3D model, the printing parameters and the resulting weights, allowing the printing of printlets with tailored weights and doses. Validating the printing process with the pharma-ink is a crucial step when using the M3DIMAKER Studio™ software. The software established a relationship between a scaled 3D model and the weight of the printlets arranged in 5 rows. To establish a correlation, printlets with different sizes were weighed, and the mean per row was calculated. Using internal algorithms, the software created a library of 3D scale models corresponding to the different weights or doses. This allows users to select the desired dose or weight, and the software automatically selects the appropriate file. The validation process is essential when new pharma-inks are used, since each pharma-ink exhibits different rheological properties that could affect the deposition of the material. Therefore, the weight assigned to the scaled 3D model may vary.

3.2. 3DP process and mass uniformity test

Batches of 28 printlets per dose (1 mg, 2 mg, and 3 mg) were successfully printed at 50 °C (Fig. 2). No obstructions of the printhead nozzle occurred during the printing process. The pharma-ink rapidly solidified when deposited during manufacture without requiring additional cooling, and the resulting printlets exhibited satisfactory handling properties. The speed of the process was prioritised over printlet resolution to ensure high throughput. Therefore, a wide 1.2 mm diameter tip and a high printing speed of 15 mm/s were selected. Consequently, the time taken to print and weigh the 1 mg, 2 mg, and 3 mg printlets were 50 s, 65 s, and 75 s, respectively.

During the printing process the printlets were individually weighed using the integrated balance of the pharmaceutical printer and the M3DIMAKER Studio™ software (Fig. 3). After the 3DP process, each printlet was weighed again to evaluate the differences between the weight measured and reported by the software (Integrated balance) and the weight manually obtained after the 3DP process in the external balance (External balance) (Table 2).

The printlet height was found to be considerably smaller when compared to the theoretical values reported in Table 1. This can be attributed to the fact that the chosen infill density (20%) resulted in gaps within the dosage forms. Therefore, the extruded material was deposited into the holes of the previous layers, reducing the overall printlet height. In addition, the width of all printlets were slightly lower than the theoretical values, which could be explained by the low printing resolution as a result of the large nozzle diameter (1.2 mm). It could be also observed that the CV decreased as the size of the printed object increased. There was less variation in the weight of the 3 mg dose printlets (CV = 1.94% or 1.93%) than in the 1 mg dose printlets (CV = 2.40% or 2.46%). This may be attributed to the lower dimensions of the 1 mg dose printlets and the relatively big diameter of the nozzle used in this study (1.2 mm).

No significant differences were found between the weights in the 3D printer balance and the external balance ($\alpha < 0.05$). According to the Ph. Eur., it is necessary to individually weigh 20 solid dosage forms and

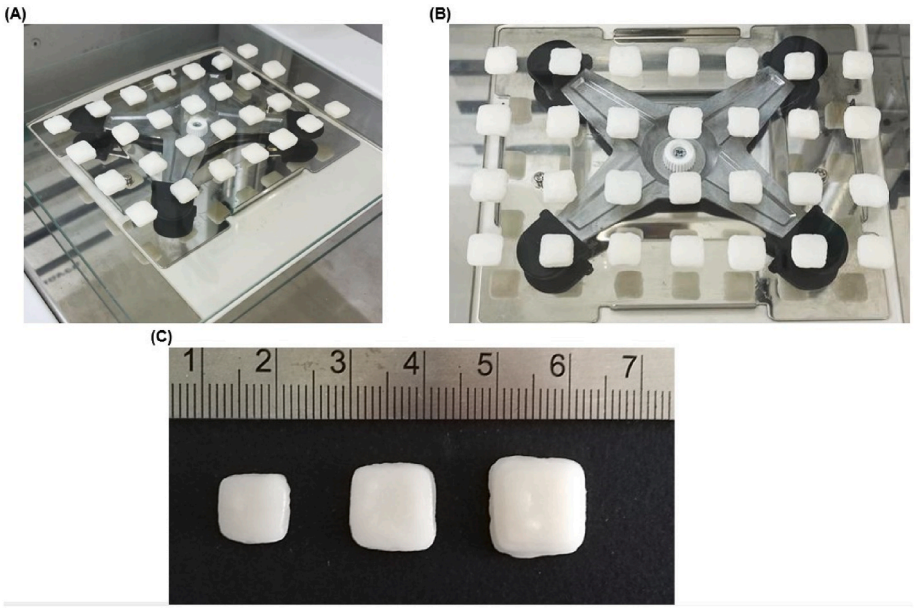

Fig. 2. Photographs of the (A) Side view of 3 mg printlets on the balance-3D printer system; (B) Top view of 3 mg printlets on the balance-3D printer system; (C) Printlets containing 1 mg, 2 mg and 3 mg (left to right). Scale in cm.

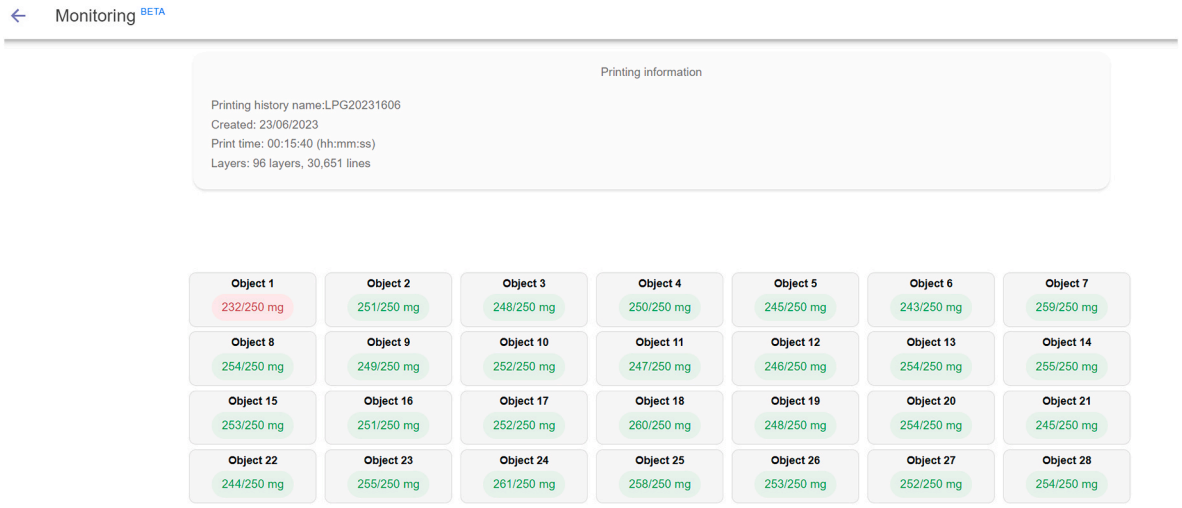

Fig. 3. Screenshots of the M3DIMAKER Studio™ software, showing the mass results obtained during the 3DP process using the integrated balance for 1 mg printlets. Accepted limits (±5% error) for the mass uniformity assay are shown in green. Samples that are not within the accepted limits are shown in red. (For interpretation of the references to colour in this figure legend, the reader is referred to the Web version of this article.)

Table 2
Dimensions and weight results of each printed batch. Results are showed as mean ± standard deviation (n = 28). CV is referred to as the Coefficient of Variation and was calculated by dividing the standard deviation by the mean weight.

Batch	Width (mm)	Height (mm)	Integrated balance weight (mg)	CV integrated balance weight (%)	External balance weight (mg)	CV external balance weight (%)
1 mg	7.71 ± 0.81	1.75 ± 0.59	250.89 ± 6.03	2.40	251.75 ± 6.19	2.46
2 mg	10.07 ± 0.81	2.68 ± 0.48	501.36 ± 11.38	2.27	502.11 ± 11.28	2.25
3 mg	11.11 ± 0.63	2.86 ± 0.45	742.46 ± 14.42	1.94	742.00 ± 14.34	1.93

determine the average mass. Fig. 4 shows the accepted deviation of the mean mass (±5%) as green dashed lines parallel to the X axis, and the individual weight distributions of each printlet during the printing process.

As observed in Fig. 4, the developed software was capable of registering the weights of all individual printlets after printing and accurately detecting any deviations within the accepted limits. For tablets of mean weight ≥250 mg (1 mg dose), only one printlet from the entire batch was outside the accepted ± 5% limits (Fig. 4A). The weight deviation was automatically registered by the M3DIMAKER Studio™ software during printing and Object 1 was marked as red (Fig. 3). Normally, the first printlet (Object 1) is not representative of the entire batch, as a result of possible air pockets in the syringe during loading or inconsistent pharma-ink flow. This is evident in Object 1 of all three batches (232/

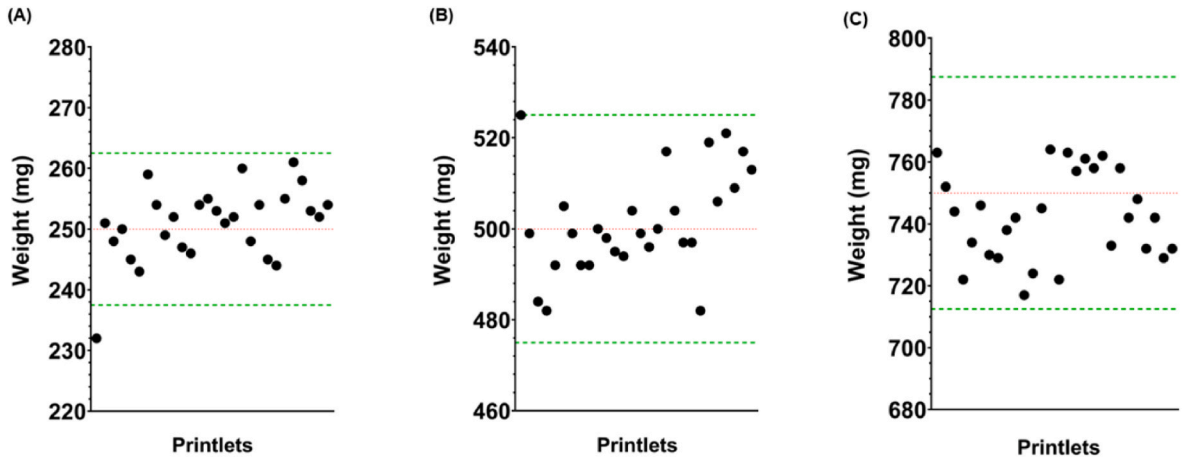

Fig. 4. Registered weights by the balance-3D printer system during the printing process: (A) 1 mg batch, (B) 2 mg batch and (C) 3 mg batch. The red line shows the declared average weight (250 mg, 500 mg, and 750 mg, respectively). The green lines show the accepted limits (±5%) (n = 28). (For interpretation of the references to colour in this figure legend, the reader is referred to the Web version of this article.)

250 mg, 525/500 mg, and 763/750 mg), with a significant deviation from the target printlet weight (Fig. 3). The deviation is detected by the software in the 1 mg batch but not in the other batches because they were inside the ±5% variation limit. The smallest accepted weight range is for the 1 mg batch, meaning slighter deviations in weight will be detected by the software as outside of the specifications. Such findings highlight the feasibility of integrating the balance as a weight control system in the 3D printer. The M3DIMAKER Studio™ software can accelerate the time-consuming quality control assay required for solid dosage forms, as it was able to detect weight deviations during the 3DP process, with no significant differences found between the weight registered by the balance-3D printer system and the external balance.

3.3. Characterization of printlets

3.3.1. XRPD and DSC

DSC and XRPD analyses were performed to determine the solid-state structure of hydrocortisone in the printlets. Pure hydrocortisone and pure Gelucire 50/13 had a melting point at 225 °C and 50 °C, respectively (Fig. 5A). The absence of this endothermic peak in the DSC thermograms of the printlets and the pharma-ink suggests that hydrocortisone was amorphous and completely dissolved in the formulation and was molecularly dispersed in the obtained printlets and pharma-ink. However, the absence of the hydrocortisone endothermic peak could also be explained by the low drug content (0.4 % w/w) and the limit of detection of both XRPD and DSC techniques. Therefore, the complete solubilization of hydrocortisone cannot be proven, but due to the pharma-ink formulation process this is highly likely [61]. Interestingly, a splitting of the Gelucire 50/13 endothermic peak at 50 °C was found, resulting in a very broad endotherm. This can be explained by the presence of different polymorphs, which are melting at different temperatures [62]. This peak splitting is more pronounced in the pharma-ink and three printlets, most likely because of the melting-cooling process during printing. The melting enthalpies (ΔHm) for the pharma-ink and printlets were measured by integrating the peaks using TA Instruments Universal Analysis 2000 (version 4.5.0.5) software and the contribution of pure Gelucire 50/13 to the melting enthalpy was calculated, considering the 89.6% w/w of pure Gelucire 50/13 in the final formulation (Table 3). The Gelucire 50/13 contribution was calculated by multiplying the Gelucire 50/13% in the final formulation (89.6 % w/w) and ΔHm.

As observed in Table 3, the pure Gelucire 50/13 contribution to the pharma-ink and printlets melting enthalpy was between 84 and 93%, indicating that the majority of pure Gelucire 50/13 contributed to the melting enthalpy.

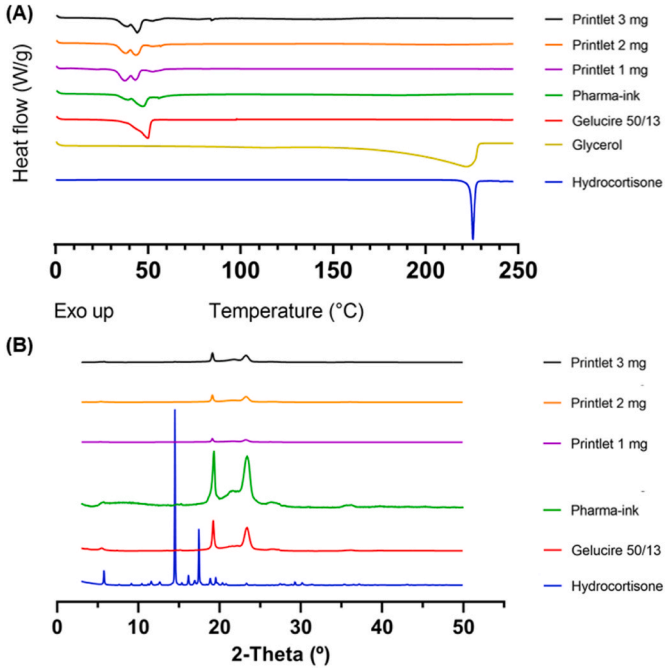

Fig. 5. (A) DSC thermograms of pure hydrocortisone and excipients, pharma-ink and different dose printlets; (B) X-ray powder diffractograms of pure hydrocortisone and excipients, pharma-ink and different dose printlets.

Table 3
Results of melting enthalpies of pure Gelucire 50/13, pharma-ink and the different printlets.

Sample	ΔHm (J/g)	Gelucire 50/13 contribution (J/g)	Gelucire 50/13 contribution (%)
Gelucire 50/13	143.7	128.8	100
Pharma-ink	134.2	120.2	93.4
Printlet 1 mg	124	111.1	86.3
Printlet 2 mg	120.4	107.9	83.8
Printlet 3 mg	124.9	111.9	86.9

As observed in the x-ray diffractograms (Fig. 5B), the peaks at 5°, 19°, and 23° 2θ can be attributed to Gelucire 50/13. The peak intensity varies for each hydrocortisone dose, explained by the fact that each

printlet was produced from a different pharma-ink, resulting in inter-batch variability. Hydrocortisone peaks cannot be seen in the pharma-ink or printlet diffractograms, due to the drug loading (0.4 % w/w) being below the detection limit of the instrument.

3.3.2. FTIR

FTIR was performed to elucidate any possible chemical interactions between hydrocortisone and the excipients (Gelucire 50/13 and glycerol) during the printing process (Fig. 6).

The spectrum suggests that there were no chemical interactions between the drug and the excipients. All the bands present in the printlets and pharma-ink can be attributed to the presence of Gelucire 50/13 due to the higher percentage in the formulation (89.6% w/w). It is possible that the drug peaks have overlapped with the characteristic bands of the Gelucire 50/13. However, because of the drug loading being below the limit of detection of the instrument, it is not possible to conclude this.

3.3.3. Drug content

The hydrocortisone content of the different printed batches (1, 2, and 3 mg) and the drug loading of the pharma-ink is reported in Table 4. The hydrocortisone content was 100% and the calculated drug loading was close to the theoretical load of 0.400% w/w.

According to the Ph. Eur., the content uniformity test of single-dose preparations is based on the assessment of the individual content of the drug of the single-dose units, to determine if the individual contents are within the established limits with respect to the average claimed. Using an appropriate analytical method, the individual drug content in 10 samples taken at random must be determined. In this study, individual content of all printlets prepared per batch (n = 28) was evaluated using the HPLC method described in Section 2.7., to determine any significant deviations in the content of each printlet. The Ph. Eur. states that the batch is accepted if each individual content is between 85% and 115% of the average content. The batch does not comply with the assay if more than one individual content is outside these limits or if one individual content is outside the limits 75%–125% of the mean content. All the printed batches in this study were between the accepted limits, and the hydrocortisone content in the pharma-ink was 100% for all the batches (**Table 4**). This ensures that all the 3D printed formulations contained the declared amount of hydrocortisone and that there was no drug degradation during printing.

Table 4
Hydrocortisone content and drug loading results performing in the different printed batches of 1 mg, 2 mg and 3 mg. mean ± standard deviation (n = 28).

Batch	Drug loading (% w/w)
1 mg	0.400 ± 0.008
2 mg	0.408 ± 0.012
3 mg	0.395 ± 0.010

3.3.4. In vitro release study

Hydrocortisone release from the printlets is shown in Fig. 7. The dissolution mechanism was erosion, and the drug was progressively released from the dosage form as it eroded. It was observed that the release from the 1 mg printlets was slightly faster than 2 mg or 3 mg due to the dosage form size. Each dosage form has a different surface area to volume ratio because of the different dimensions (1 mg–1.11 cm^{-1}; 2 mg–0.92 cm^{-1}; 3 mg–0.80 cm^{-1}), resulting in a slightly different drug release rate. Approximately 58% (1 mg printlet), 54% (2 mg printlet) and 48% (3 mg printlet) of the drug was released at 60 min. It can be observed in Fig. 7 that 95% of the hydrocortisone was released after 135min (independent of the surface area to volume ratio).

According to the Ph. Eur., conventional immediate release dosage forms should release at least 75% of the active substance within a specified time, typically 45 min or less [63]. However, only ~ 50%, 47% and 43% of hydrocortisone was released from printlets 1 mg, 2 mg, and 3 mg, respectively, at 45 min. Therefore, the printlets cannot be considered immediate release dosage forms.

The balance-3D printer system accelerated, in terms of time and human resources, the mass uniformity assay which is mandatory for solid dosage forms according to the European and United States Pharmacopoeias. The content uniformity of the three batches was approximately 100% and hydrocortisone was completely released. However, the weight system may not be enough to assure the overall quality of the batches. In this work, the content uniformity to assure the correct dose was performed using a destructive method of analysis (HPLC). This is

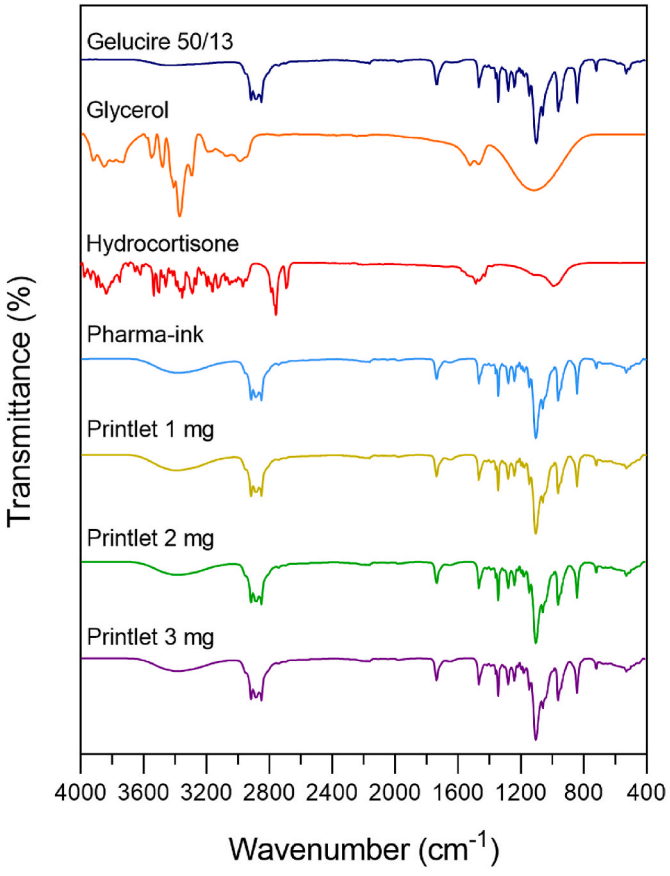

Fig. 6. FTIR spectra of Gelucire 50/13, glycerol, pure hydrocortisone, pharma-ink and printlets with varying hydrocortisone dose.

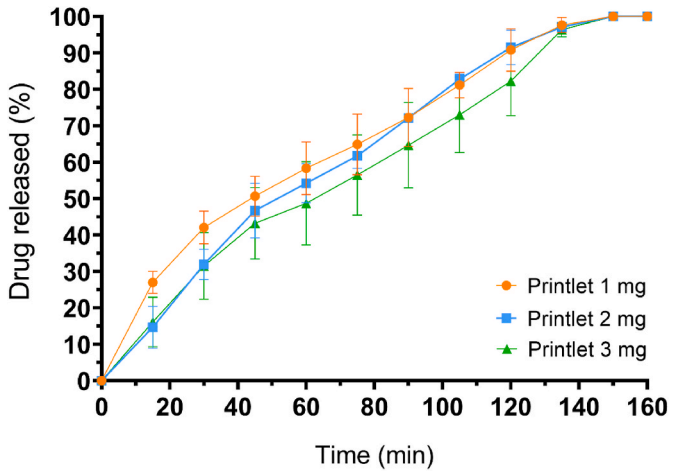

Fig. 7. Hydrocortisone dissolution profiles from 1 mg, 2 mg and 3 mg printlets.

not ideal, especially when preparing small, customized batches for specific patients, as more dosage forms would have to be printed than necessary to carry out the content uniformity test. To date, NIR spectroscopy has been investigated as an alternative tool to quantify the drug loading of 3D printed dosage forms and even the density and drug release from printlets, avoiding destructive techniques [48,49,53,64]. An in-line NIR system was investigated to perform real-time drug content analysis of efavirenz-loaded printlets prepared using pharma-inks produced by a pharmaceutical company [26]. Portable NIR equipment has also been used as a PAT tool for quantifying timolol maleate printed on contact lenses [48], amlodipine and lisinopril polyprintlets [52], caffeine printlets [49], and hydrocortisone printlets [53]. In addition, NIR hyperspectral imaging (NIR-HSI) was used as a PAT tool to monitor and quantify the amount of metformin hydrochloride printed onto films [51]. The studies showed a good correlation with the reference method (HPLC). Therefore, it was demonstrated that NIR could be a low-cost, non-destructive, feasible, accurate and rapid method for quality control and drug loading verification.

The next step could be the integration of a software-controlled NIR device into the balance-3D printer system, providing both mass uniformity and content uniformity in-line testing. The combination of NIR and the analytical balance into the pharmaceutical 3D printer would assure the overall quality of the batches. Another option could be the verification and validation of the correct drug content in the previously prepared pharma-ink loaded cartridges. However, the correct drug content of each final 3D printed dosage form would still need to be ensured to demonstrate no degradation or loss of drug during printing and post-printing.

4. Conclusions

This is the first study to investigate the implementation of an in-line, software-controlled, analytical balance within a pharmaceutical 3D printer. Automated mass uniformity testing was carried out on three batches (n = 28) of SSE 3D printed formulations of hydrocortisone in three different doses (1, 2, and 3 mg). The specialised integrated software was capable of successfully registering the weight of each printlet and detecting any deviations from the accepted ±5% limits. Only one printlet from all three batches was outside the accepted range, and the weight deviation was immediately registered by the software and the object was rejected. The weights obtained were compared against an external analytical balance, and no significant differences were found between the registered weights. Overall, this study highlights the feasibility of integrating an in-line balance as an accurate and automatic weight control system in the 3D printer. The use of specialised and validated software can speed up and automate the weight uniformity quality control process for the entire batch, ensuring that 3DP of medicines meets the strict regulatory quality control requirements.

CRediT authorship contribution statement

Carlos Bendicho-Lavilla: Conceptualization, Data curation, Formal analysis, Investigation, Methodology, Software, Writing – original draft, Writing – review & editing. **Lucía Rodríguez-Pombo:** Data curation, Formal analysis, Funding acquisition, Investigation, Methodology, Writing – original draft, Writing – review & editing. **Patricija Januskaite:** Formal analysis, Project administration, Validation, Writing – original draft, Writing – review & editing. **Carlos Rial:** Conceptualization, Investigation, Methodology, Software, Validation. **Carmen Alvarez-Lorenzo:** Conceptualization, Formal analysis, Funding acquisition, Investigation, Project administration, Resources, Supervision, Validation, Visualization, Writing – review & editing. **Abdul W. Basit:** Conceptualization, Project administration, Resources, Supervision, Validation, Visualization, Writing – review & editing. **Alvaro Goyanes:** Conceptualization, Funding acquisition, Investigation, Project administration, Resources, Supervision, Validation, Visualization, Writing – review & editing.

Declaration of competing interest

The authors declare the following financial interests/personal relationships which may be considered as potential competing interests: The authors declare the following financial interests/personal relationships which may be considered as potential competing interests. Alvaro Goyanes and Abdul Basit are co-founders and directors at FabRx. Both Carlos Bendicho-Lavilla and Carlos Rial are employees of FabRx.

Data availability

Data will be made available on request.

Acknowledgments

LRP acknowledges the predoctoral fellowship [FPU20/01245] provided by the Ministerio de Universidades [Formación de Profesorado Universitario (FPU 2020)].

References

[1] S. Wang, et al., A review of 3D printing technology in pharmaceutics: technology and applications, now and future, Pharmaceutics 15 (2) (2023).
[2] T. Tracy, et al., 3D printing: innovative solutions for patients and pharmaceutical industry, Int. J. Pharm. 631 (2023) 122480.
[3] R. Govender, et al., Polymers in pharmaceutical additive manufacturing: a balancing act between printability and product performance, Adv. Drug Deliv. Rev. 177 (2021) 113923.
[4] L.A. Junqueira, et al., Coupling of fused deposition modeling and inkjet printing to produce drug loaded 3D printed tablets, Pharmaceutics 14 (2022), https://doi.org/10.3390/pharmaceutics14010159.
[5] X. Xu, et al., Smartphone-enabled 3D printing of medicines, Int. J. Pharm. 609 (2021) 121199.
[6] L. Rodríguez-Pombo, et al., Simultaneous fabrication of multiple tablets within seconds using tomographic volumetric 3D printing, Int. J. Pharm. X 5 (2023) 100166.
[7] J.J. Ong, et al., Supramolecular chemistry enables vat photopolymerization 3D printing of novel water-soluble tablets, Int. J. Pharm. 643 (2023) 123286.
[8] A. Ghanizadeh Tabriz, et al., 3D printing of LEGO® like designs with tailored release profiles for treatment of sleep disorder, Int. J. Pharm. (2023) 122574.
[9] F. Wang, et al., Development of pH-responsive polypills via semi-solid extrusion 3D printing, Bioengineering (Basel) 10 (4) (2023).
[10] K. Chachlioutaki, et al., Quality control evaluation of paediatric chocolate-based dosage forms: 3D printing vs mold-casting method, Int. J. Pharm. 624 (2022) 121991.
[11] I. Seoane-Viaño, et al., Visualizing disintegration of 3D printed tablets in humans using MRI and comparison with in vitro data, J. Contr. Release 365 (2023) 348–357.
[12] K. Englezos, et al., 3D printing for personalised medicines: implications for policy and practice, Int. J. Pharm. 635 (2023) 122785.
[13] N. Beer, et al., Magistral compounding with 3D printing: a promising way to achieve personalized medicine, Ther Innov Regul Sci 57 (1) (2023) 26–36.
[14] Andreadis II, et al., The advent of a new era in digital healthcare: a role for 3D printing technologies in drug manufacturing? Pharmaceutics 14 (3) (2022).
[15] A. Awad, et al., A review of state-of-the-art on enabling additive manufacturing processes for precision medicine, J. Manuf. Sci. Eng. 145 (1) (2022).
[16] M.A. Azad, et al., Polymers for extrusion-based 3D printing of pharmaceuticals: a holistic materials-process perspective, Pharmaceutics 12 (2) (2020).
[17] F. Fina, et al., 3D printing of tunable zero-order release printlets, Polymers 12 (8) (2020) 1769.
[18] M. Uboldi, et al., Investigation on the use of fused deposition modeling for the production of IR dosage forms containing Timapiprant, Int. J. Pharm. X 5 (2023) 100152.
[19] J. Macedo, et al., Influence of formulation variables on the processability and properties of tablets manufactured by fused deposition modelling, Int. J. Pharm. 637 (2023) 122854.
[20] M. Pistone, et al., Direct cyclodextrin based powder extrusion 3D printing of budesonide loaded mini-tablets for the treatment of eosinophilic colitis in paediatric patients, Int. J. Pharm. 632 (2023) 122592.
[21] J. Boniatti, et al., Direct powder extrusion 3D printing of praziquantel to overcome neglected disease formulation challenges in paediatric populations, Pharmaceutics 13 (8) (2021).
[22] J.J. Ong, et al., 3D printed opioid medicines with alcohol-resistant and abuse-deterrent properties, Int. J. Pharm. 579 (2020) 119169.
[23] A. Awad, et al., 3D printed infliximab suppositories for rectal biologic delivery, Int. J. Pharm. X 5 (2023) 100176.

[24] L. Rodríguez-Pombo, et al., Innovations in chewable formulations: the novelty and applications of 3D printing in drug product design, Pharmaceutics 14 (2022), https://doi.org/10.3390/pharmaceutics14081732.
[25] I. Seoane-Viaño, et al., 3D printed tacrolimus rectal formulations ameliorate colitis in an experimental animal model of inflammatory bowel disease, Biomedicines 8 (12) (2020).
[26] I. Seoane-Viaño, et al., A case study on decentralized manufacturing of 3D printed medicines, Int. J. Pharm. X 5 (2023) 100184.
[27] I. Seoane-Viaño, et al., Semi-solid extrusion 3D printing in drug delivery and biomedicine: personalised solutions for healthcare challenges, J. Contr. Release 332 (2021) 367–389.
[28] B. Zhang, et al., An investigation into the effects of ink formulations of semi-solid extrusion 3D printing on the performance of printed solid dosage forms, J. Mater. Chem. B (2024).
[29] J. Johannesson, et al., Quality attributes for printable emulsion gels and 3D-printed tablets: towards production of personalized dosage forms, Int. J. Pharm. 646 (2023) 123413.
[30] A.T. Chatzitaki, et al., Fabrication of 3D-printed octreotide acetate-loaded oral solid dosage forms by means of semi-solid extrusion printing, Int. J. Pharm. 632 (2023) 122569.
[31] I.E. Aita, J. Breitkreutz, J. Quodbach, Investigation of semi-solid formulations for 3D printing of drugs after prolonged storage to mimic real-life applications, Eur. J. Pharmaceut. Sci. 146 (2020) 105266.
[32] S. Abdella, et al., 3D printing of thermo-sensitive drugs, Pharmaceutics 13 (2021), https://doi.org/10.3390/pharmaceutics13091524.
[33] T. Jiang, et al., Extrusion bioprinting of soft materials: an emerging technique for biological model fabrication, Appl. Phys. Rev. 6 (1) (2019) 011310.
[34] J. Wang, Z. Cui, M. Maniruzzaman, Bioprinting: a focus on improving bioink printability and cell performance based on different process parameters, Int. J. Pharm. 640 (2023) 123020.
[35] A.G. Tabriz, et al., Personalised tasted masked chewable 3D printed fruit-chews for paediatric patients, Pharmaceutics 13 (8) (2021) 1301.
[36] E. Sjöholm, et al., Semi-solid extrusion 3D printing of tailored ChewTs for veterinary use - a focus on spectrophotometric quantification of gabapentin, Eur. J. Pharmaceut. Sci. 174 (2022) 106190.
[37] T.T. Yan, et al., Semi-solid extrusion 3D printing ODFs: an individual drug delivery system for small scale pharmacy, Drug Dev. Ind. Pharm. (2020) 1–8.
[38] P. Panraksa, et al., Hydroxypropyl methylcellulose E15: a hydrophilic polymer for fabrication of orodispersible film using syringe extrusion 3D printer, Polymers 12 (2020), https://doi.org/10.3390/polym12112666.
[39] E. Utomo, et al., Development of 3D-printed vaginal devices containing metronidazole for alternative bacterial vaginosis treatment, Int. J. Pharm. X 5 (2023) 100142.
[40] J. Rahman-Yildir, B. Fischer, J. Breitkreutz, Development of sustained-release drug-loaded intravesical inserts via semi-solid micro-extrusion 3D-printing for bladder targeting, Int. J. Pharm. 622 (2022) 121849.
[41] FDA. *CURRENT GOOD MANUFACTURING PRACTICE FOR FINISHED PHARMACEUTICALS*, 2023. Available from, https://www.accessdata.fda.gov/scripts/cdrh/cfdocs/cfcfr/CFRSearch.cfm?CFRPart=211.
[42] A. Goyanes, et al., Automated therapy preparation of isoleucine formulations using 3D printing for the treatment of MSUD: first single-centre, prospective, crossover study in patients, Int. J. Pharm. 567 (2019) 118497.
[43] M. Lyousoufi, et al., Development and bioequivalence of 3D-printed medication at the point-of-care: bridging the gap toward personalized medicine, Clin. Pharmacol. Therapeut. 113 (5) (2023) 1125–1131.
[44] D. Markl, et al., Toward quality assessment of 3D printed oral dosage forms, Journal of 3D Printing in Medicine 2 (1) (2017) 27–33.
[45] (USP), T.U.S.P, Uniformity of dosage units, Available from, https://www.usp.org/sites/default/files/usp/document/harmonization/excipients/m99694.pdf, 2022.
[46] A.K. Jørgensen, et al., Advancing non-destructive analysis of 3D printed medicines, Trends Pharmacol. Sci. 44 (6) (2023) 379–393.
[47] E. Díaz-Torres, et al., Integrating pressure sensor control into semi-solid extrusion 3D printing to optimize medicine manufacturing, Int. J. Pharm. X 4 (2022) 100133.
[48] T.D. Pollard, et al., Inkjet drug printing onto contact lenses: deposition optimisation and non-invasive dose verification, Int. J. Pharm. X 5 (2023) 100150.
[49] T.L. Yang, et al., The use of near-infrared as process analytical technology (PAT) during 3D printing tablets at the point-of-care, Int. J. Pharm. 642 (2023) 123073.
[50] S.J. Trenfield, et al., Prediction of solid-state form of SLS 3D printed medicines using NIR and Raman spectroscopy, Pharmaceutics 14 (3) (2022).
[51] S. Stranzinger, et al., Near-infrared hyperspectral imaging as a monitoring tool for on-demand manufacturing of inkjet-printed formulations, AAPS PharmSciTech 22 (6) (2021) 211.
[52] S.J. Trenfield, et al., Non-destructive dose verification of two drugs within 3D printed polyprintlets, Int. J. Pharm. 577 (2020) 119066.
[53] T.L. Yang, et al., Towards point-of-care manufacturing and analysis of immediate-release 3D printed hydrocortisone tablets for the treatment of congenital adrenal hyperplasia, Int. J. Pharm. 642 (2023) 123072.
[54] J. Madathilethu, et al., Content uniformity of quartered hydrocortisone tablets in comparison with mini-tablets for paediatric dosing, BMJ paediatrics open 2 (1) (2018) e000198-e000198.
[55] S. Ayyoubi, et al., 3D printed, personalized sustained release cortisol for patients with adrenal insufficiency, Int. J. Pharm. 630 (2023) 122466.
[56] K. Vithani, et al., A proof of concept for 3D printing of solid lipid-based formulations of poorly water-soluble drugs to control formulation dispersion kinetics, Pharmaceut. Res. 36 (7) (2019) 102.
[57] D. Nisticò, et al., Pediatric adrenal insufficiency: challenges and solutions, Therapeut. Clin. Risk Manag. 18 (2022) 47–60.
[58] D. El-Maouche, W. Arlt, D.P. Merke, Congenital adrenal hyperplasia, Lancet 390 (10108) (2017) 2194–2210.
[59] H. Hoyer-Kuhn, et al., Hydrocortisone dosing in children with classic congenital adrenal hyperplasia: results of the German/Austrian registry, Endocr Connect 10 (5) (2021) 561–569.
[60] C.J. Watson, et al., Pharmaceutical compounding: a history, regulatory overview, and systematic review of compounding errors, J. Med. Toxicol. 17 (2) (2021) 197–217.
[61] I. Lafeber, et al., 3D printed furosemide and sildenafil tablets: innovative production and quality control, Int. J. Pharm. 603 (2021) 120694.
[62] A.A. Date, et al., Lipid nanocarriers (GeluPearl) containing amphiphilic lipid Gelucire 50/13 as a novel stabilizer: fabrication, characterization and evaluation for oral drug delivery, Nanotechnology 22 (27) (2011) 275102.
[63] (EMA), E.M.A, Reflection paper on the dissolution specification forgeneric solid oral immediate release products with systemic action, Available from, https://www.ema.europa.eu/en/documents/scientific-guideline/reflection-paper-dissolution-specification-generic-solid-oral-immediate-release-products-systemic-action-first-version_en.pdf, 2017.
[64] S.J. Trenfield, et al., Releasing fast and slow: non-destructive prediction of density and drug release from SLS 3D printed tablets using NIR spectroscopy, Int. J. Pharm. X 5 (2023) 100148.